An Analysis of FPGA Enabled Magnetic Sensor based Automatic Beam Tracking System for Wireless Power Transfer System in Brain Implant

Nabanita Saha, Erik Pineda-Alvarez, Ifana Mahbub
The University of Texas at Dallas, USA

***Abstract* — This paper presents an Field Programmable Gate Array (FPGA) enabled magnetic sensor based automatic beam tracking method for a phased array based wireless power transfer system to be implemented in brain implant. This method is proposed to track the position of the receiver (placed on the head of a freely moving rodent) and steer the beam of the transmitter phased-array towards the direction instantaneously. The coordinate locations of the target are obtained from the magnetic sensor and read-out circuit and an algorithm is proposed that converts the magnetic sensor read-out signal to the corresponding digital bit configuration of the phase shifters of the phased-array transmitter. The analysis show that the power transfer efficiency is higher (9.09%) when the rodent is in static condition compared to the dynamic condition (5.4%). It also shows that the PTE degrades (5.09%) as the steered beam goes into the blind spot. The process of tracking the target and focusing of the beam has been validated with measurement.**

***Keywords* — ceramics, coaxial resonators, delay filters, power amplifiers.**

I. Introduction

With the advancements made on wireless power transfer (WPT) systems, transferring continuous power to low-power circuits such as implantable medical devices is becoming more prevalent in biomedical applications. The recent advancements in antenna miniaturization, circuit design, and bio-compatible materials are opening up new opportunities for subtle diagnosis of disease using wireless implantable devices [1]. In WPT system where the location of the receiver changes with time, such as in neuroscience-related experiment or mobile devices such as UAVs (Unmanned Aerial Vehicle), it is important to track the target to reduce the power loss due to beam misalignment. There are several target detection methods that have been proposed in prior works, for example radar-based positioning system [2], optical-based positioning system [3], acoustic-based localization [4], etc. but these methods are not suitable for near-field WPT systems due limitations such as spatial resolution, line-of-sight requirements, etc.

One of the commonly adopted WPT tracking system is retro-directive technology [5]-[6]. In retro-directive technology, the receiver emits a pilot signal which enables the transmitter to determine the receiver's direction. After estimating the receivers location, the transmitter sends the microwave beam toward the receiver's direction. The drawback of retro-directive technology is that the receiver must use energy to send a pilot signal. This method is not suitable to apply in cases such as IoT devices without batteries or mobile phones without electricity. WPT system has become one of the most popular methods for headstage-based neural stimulation in recent times [7]. Due to the rodents free movement, the location of the receiver is not static. In our prior work a phased-array antenna-based near-field radioactive WPT system was developed where the power beam can be steered electronically towards the headstage of the freely moving rodent [5]. The limitation of this proposal is that it cannot detect the location of the receiver. To overcome this challenge, here we proposed an automatic beam tracking system with FPGA driven hardware implementation that can detect the position of the receiver using a magnet sensor and steer a focused beam towards the direction of the implant. The target position of the receiver is estimated in real-time by defined sections made by the magnet sensor.

The novelty of this proposed work is- *i)* Development and implementation of an algorithm for an automatic beam tracking system, *ii)* Tracking the location for the receiver in various angular and linear distances with minimum error, and *iii)* Analysis of the power transfer efficiencies (PTE) in the receiver plane for difference cases.

II. System Overview

The proposed WPT technology consists of two parts, the microwave power beamforming module and the automatic receiver location detection module. The microwave power beamforming module consists of a 2.4 GHz phased array transmitter antenna, and four phase shifters two of which are 4-bit (APS-010144 by Macom) and the other two are 5-bit phase shifters (CMD175P4 by Qorvo). The fundamental components of the automatic receiver location detection module are: a magnet mounted with the receiver placed in the headstage of the freely moving animal, while the transmitter components consist of the magnetic sensor, Nexys A7: FPGA Trainer Board, and the phase shifters for the beam forming system. The overall system diagram of the proposed closed-loop magnetic sensor based tracking integrated WPT system is presented in Fig. 1(a).

In the proposed system, the test animal is in a behavioral cage of $26 \times 23 \times 16cm^3$ dimension and the power needs to be transferred to the Rx antenna (placed in the headstage) in this area coverage. With the RX antenna of $24{\times}24$ mm^3 aperture and the TX antenna of 25° HPBW, the beam coverage area is 15.48 cm^2 it is needed to steer the beam to cover the

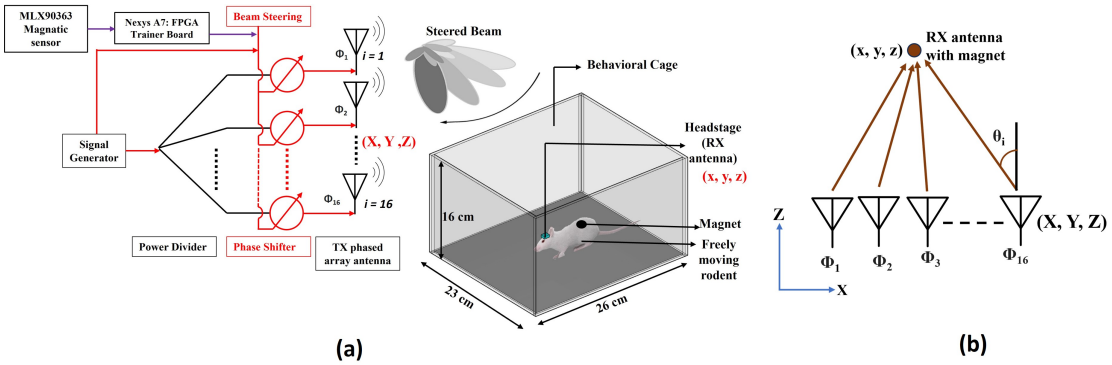

Fig. 1. (a) A 3D rendered overview of the FPGA enabled magnetic sensor based automatic beam tracking system (b) Representation of target angle in the z-direction

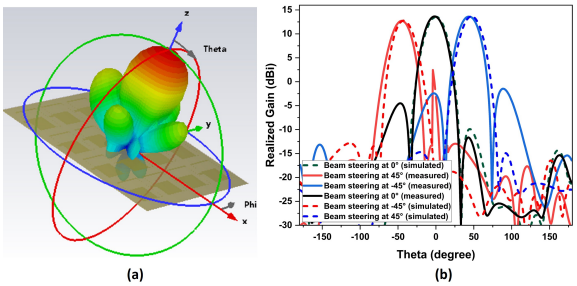

Fig. 2. (a) 3D Radiation Pattern (b) Representation of beam-steering along θ plane for different phase combinations

whole area of the cage in 10 cm distance along the z-axis. The TX antenna is placed on the top/bottom of the behavioral cage. The TX and RX antennas resonate at 2.4 GHz within the ISM band which is suitable for biomedical applications. The proposed TX antenna for this work is a 4×4 phased array antenna that is designed to transmit wireless power through a unidirectional beam [8]. The unidirectional beam reduces the power loss and focuses the power towards the receiver by directing most of the power to a single location. All of adjacent antenna elements can be set with the phase difference $\Delta\phi$. When the WPT distance is close the target angle θ with each antenna element will be different. Here, the target angle θ_i with i^{th} antenna element can be represented as follows [9]:

$$tan(\theta_i) = \frac{(x_i - X)}{(z_i - Z)} \tag{1}$$

The phase ϕ_i of the i^{th} element of the N-element array antenna in the near-field can be written as:

$$\phi_i = 2\pi \sqrt{\frac{(x_i - X)^2 + (z_i - Z)^2}{\lambda}} \tag{2}$$

In eqn.(1) and eqn.(2), (x_i, z_i) are the coordinates of the antenna element of the phased array antenna.

Phase differences are provided for the various TX antenna port to steer the unidirectional beam into different angles towards the mobile receiver, these input phases are presented in Table 1. The 3D unidirectional radiation pattern and the beam-steering results along θ plane for different phase combination is presented in Fig.2 (a) and (b), respectively. The beam steering range from -45° to 45° is adequate to cover the full area of the cage.

Table 1. Beam Steering along the θ-axis for different phases

Input phases				Beam Direction	HPBW	Gain (dBi)
Q1-Q8	Q9-Q12	Q13-Q14	Q15-Q16			
11.25°	78.25°	337.5°	45°	-45°	25.4°	13.6
45°	202.5°	135°	225°	0°	25.1°	13.1
180°	157.5°	337.5°	78.25°	45°	25.6°	12.6

III. Proposed Closed-Loop Tracking System

A. Tracking the location of the receiver

The tracking system was initially developed using an MSP432 micro-controller and the magnet sensor MLX90363 by Melexis communicating using SPI. The MLX90363 is sensitive to three (B_X, B_Y and B_Z) components of the flux density applied to the IC which allows it to sense any magnet moving in its surroundings and decode its position through appropriate signal processing. The WPT working area ranges from α_2 to $-\alpha_2$ based on the sensor range, as shown in Fig.4. The distance of the receiver from the monolithic MLX90363 Magnetometer IC is defined as r in the near-field. The target's location was indicated by a single neodymium magnet as the tracer. With proper configurations in the magnet sensor, two data variables (X and Y) are extracted. These variables are used in the location calculation, that being either Cartesian coordinates or an angle based on its location. Once the optimal data variant was chosen an FPGA has been used instead of the micro-controller for higher speeds and state defined programming, which gave way for a more responsive device.

B. Location based on Cartesian Coordinates (Point-wise)

An algorithm is developed and tested in Code Composer Studio (CCS) for this approach. The target surface location plane, which is orientated to the TX antenna, is divided into XYZ coordinates based on the direction angle of the unidirectional beam. After gathering the SPI information, the corresponding angle is computed from the XYZ data of the MSP432 micro-controller. Based on the matching of the location, it updates the GPIO outputs to steer the beam towards the target. While this approach is operational there are multiple drawbacks. One such drawback is the X value would rotate too far and give a 180 degree shift due to an internal sensor value which is incorrect. A second issue from this method is the reduction in speed as the Cartesian coordinates need to be

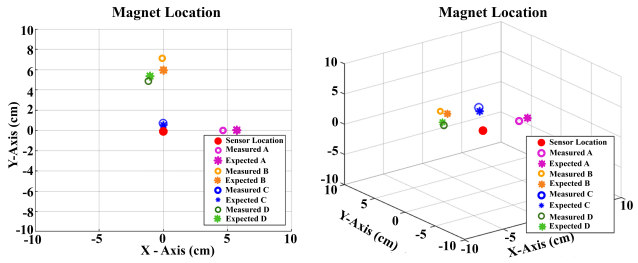

Fig. 3. Tracking the location of the magnet based on Cartesian plane (Point-wise)

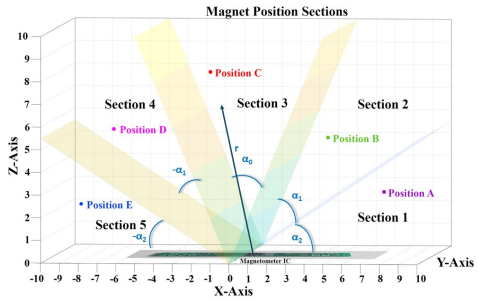

Fig. 4. Tracking the location of the magnet based on α angle (Section-wise)

converted into angles and properly matched to the TX angles. The first issue can be corrected with a digital filter however this adds to operation time which further exacerbates the second issue. The measured location of the receiver corresponding to the exact location using this approach is represented in Fig. 3.

1) *Location based on α angle (Section-wise)*

The second approach to the firmware is able to work faster with less conversions as it takes the angle calculated from the magnet sensor directly. In this approach the WPT area is divided into five angular sections based on the beam's accuracy, as shown in Fig. 4. The detailed flowchart of the auto-tracking process is illustrated in Fig.5. After initializing the FPGA and set it to the default section, the sectioned location corresponding to the receiver position is determined from the MLX90363 sensor and the micro-controller updates the phase combinations based on the α angle thus the unidirectional beam from the TX antenna is adjusted to the desired section. To further increase the speed of the device the FPGA was applied instead of a micro-controller and the sections where assigned to a digital reference table that removed the need of heavy calculations. This technique can decrease the computation time however the system does trade Y-axis accuracy for this speed.

IV. Power Transfer Efficiency Analysis

After determining the location of the receiver using the magnetic sensor, the phase combinations are updated by FPGA and the beam is steered towards the receiver. It is important to analyze the overall power transfer efficiency (PTE) in this feedback control loop system. PTE of a WPT system is the ratio of the RF output power to the RF input power for the WPT link, shown in Eqn.3. The PTE of the proposed WPT system is given by eqn. 4.

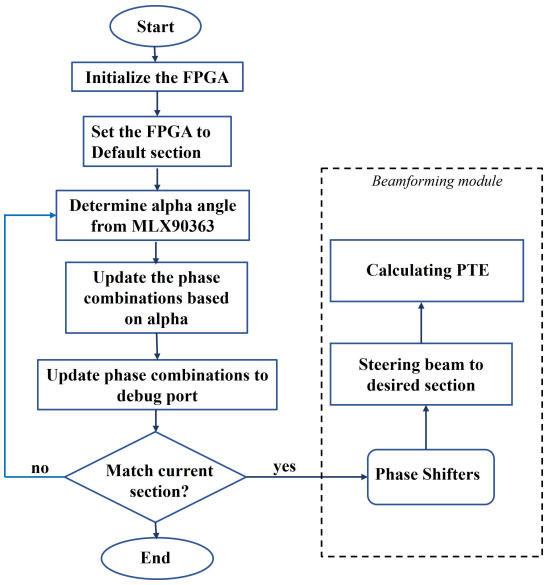

Fig. 5. Detailed flowchart of the auto-tracking process

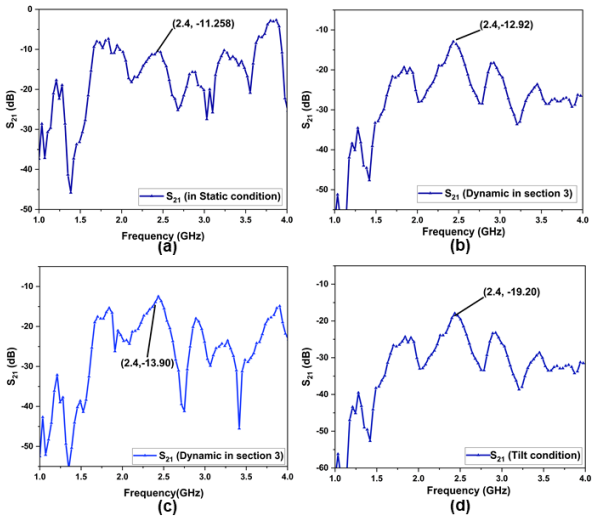

Fig. 6. S_{21} parameters in (a)static condition (b) dynamic condition in section 3 (c) dynamic condition in section 5 (d) tilted condition

$$PTE = \frac{P_{RFout}}{P_{RFin}} \times 100\% \tag{3}$$

$$\frac{P_{RFout}}{P_{RFin}} = 10^{\frac{|S_{21}|}{10}} \tag{4}$$

The beam steering along the elevation plane for different phases is shown in Table 1. In near field, the interactions between the transmitter and receiver are complex, and traditional path loss models may not be suitable. Therefore, measurements have been taken to characterize the behavior accurately.

A. *Static Location*

When the location of the receiver is static, the radiated beam can be focused towards the RX antenna. The S_{21} parameter between TX and RX is -11.25 dB at $r = 10cm$ distance apart. The results are plotted in Fig. 6(a). From the

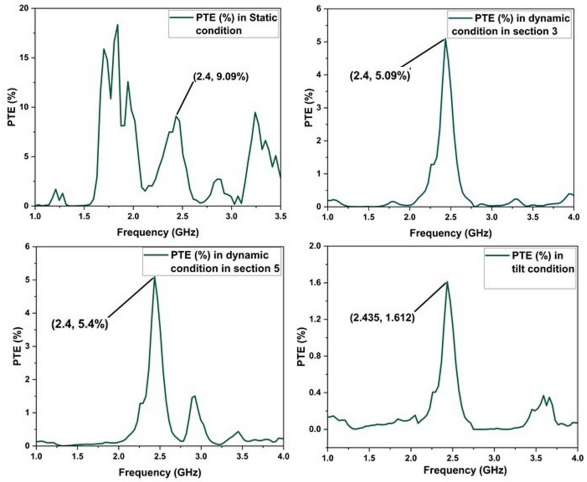

Fig. 7. Power transfer efficiency in (a) static condition, (b) dynamic condition in section 3, (c) dynamic condition in section 5, (d) tilted condition

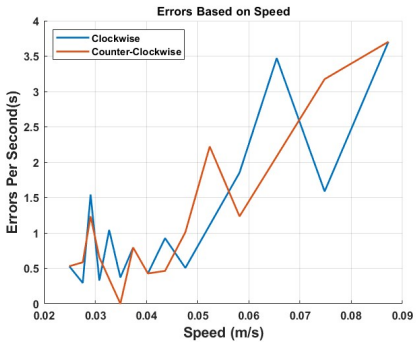

Fig. 8. % Error rate based on speed in clockwise (from $-\alpha_2$ to α_2) and counterclockwise (from α_2 to $-\alpha_2$) sections

S_{21} value, the PTE (9.09%) is calculated in the static condition which is shown in Fig. 7 (a).

B. Dynamic Location

As the rodent is a freely moving animal the location changes with time in the behavioral cage, due to this the PTE analysis becomes more complex. The analysis is implemented considering parameters such as velocity, angular distance, etc. The S_{21} in different sections are represented in Fig. 6(b) and 6(c).The S_{21} value is -12.92 dB and -13.90 dB in section 3 and section 5 respectively. The PTE in section 3 and 5 is 5.09% and 5.4% respectively shown in Fig. 7. While steering the beam in the section 1, as defined in Fig.4, and section 5 (α_2 and $-\alpha_2$), the PTE degrades as the steered beam goes into the blind spot. When transferring power to the section 2, 3 and 4, the PTE is higher compared to section 1 and 5.

C. Tilted Location

It is assumed that the alignment of the receiver will also vary as the rodent can tilt the receiver. Since, the receiver is not circularly polarized, the S_{21} between the TX and the RX antenna degrades. The PTE of the system degrades while the RX antenna is tilted, this reduction is shown in the S-parameter in Fig.7(d). The S_{21} value is -19.90 dB in the section 3 and the PTE is 1.61% while the receiver is tilted.

D. Error based on Speed

As the rodent moves speed will not remain constant and thus testing based on speed was also required. The percent error based on speed is represented in Fig. 8. The figure plots two graphs where the FPGA system was tested for the amount of times the system would fail to report the correct section at certain speeds. This graph takes the data gathered at selected speeds and normalizes the samples to one second for plotting. From the figure it is clear that as the speed increases the accuracy will decrease as shown in Fig 8. To reduce inaccuracies the FPGA was loaded with a hysteresis trigger on each section in the firmware in order to increase accuracy between neighboring sections.

V. Conclusion

A magnetic sensor based automatic beam tracking WPT system using a 4×4 phased array is designed and demonstrated in this proposed work. The system proposed in this work realizes the phase control on the X,Y and Z-axis and α angle. The detecting process provides an accurate 3D location of the receiver. In the future,there is plan to increase the steering range to get a more precise location of the receiver or more section definitions.

Acknowledgment

This material is based upon work supported by the National Science Foundation under Grant No. ECCS 2309413.

References

[1] X. Wei and J. Liu, “Power sources and electricthe al recharging strategies for implantable medical devices,” Frontiers Energy Power Eng. China, vol. 2, no. 1, pp. 1–13, 2008.

[2] M. Chiani, A. Giorgetti and E. Paolini, "Sensor Radar for Object Tracking," in Proceedings of the IEEE, vol. 106, no. 6, pp. 1022-1041, June 2018.

[3] L. Batistić and M. Tomic, "Overview of indoor positioning system technologies," 2018 41st International Convention on Information and Communication Technology, Electronics and Microelectronics (MIPRO), 2018, pp. 0473-0478.

[4] Z. Huang et al., “Position and orientation measurement system using spread spectrum sound for greenhouse robots,” Biosyst. Eng., vol. 198, pp. 50–62, Oct. 2020.

[5] D. Belo, D. C. Ribeiro, P. Pinho, and N. BorgesCarvalho, “A selective, tracking, and power adaptive far-field wireless power transfer system,” IEEE Trans. Microw. Theory Techn., vol. 67, no. 9, pp. 3856–3866, Sep. 2019.

[6] T. Mitani, S. Kawashima, and N. Shinohara, “Experimental study on a retrodirective system utilizing harmonic reradiation from rectenna,” IEICE Trans. Electron., vol. E102.C, no. 10, pp. 666–672, 2019.

[7] D. K. Biswas, N. Saha and I. Mahbub, "Wirelessly Powered 3-D Printed Headstage Based Neural Stimulation System for Optogenetic Neuromodulation Application," in IEEE Journal of Electromagnetics, RF and Microwaves in Medicine and Biology, vol. 7, no. 1, pp. 24-31, March 2023, doi: 10.1109/JERM.2022.3225972.

[8] N. Saha and I. Mahbub, "Design, Modeling, and Simulation of a 2.4GHz Near-field Phased-Array based Wireless Power Transfer System for Brain Neuromodulation Applications," 2022 IEEE Texas Symposium on Wireless and Microwave Circuits and Systems (WMCS), 2022, pp. 1-5.

[9] B. Yang, T. Mitani and N. Shinohara, "Auto-Tracking Wireless Power Transfer System With Focused-Beam Phased Array," in IEEE Transactions on Microwave Theory and Techniques, vol. 71, no. 5, pp. 2299-2306, May 2023, doi: 10.1109/TMTT.2022.3222179.